Ductile Components of Phosphorous-Alloyed P/M Steel

Jean Lynn, Paulo Rosa, DaimlerChrysler Corporation
Harry Meyer III, H.T. Mat'ls Lab, Oak Ridge National Lab
Ulf Engstrom, North American Hoganas and
Sigurd Berg, Jan Tengzelius, Ola Bergman, Robert Frykholm, Höganäs AB

World Congress on Powder Metallurgy & Particulate Materials
June 16-21, 2005, Montreal, Canada

ABSTRACT

Phosphorus is an extensively used additive in ferrous Powder Metallurgy components for magnetic applications. Changes in powders and /or sintering processes, however, occasionally lead to intergranular cracking in parts made from phosphorus-containing materials. The goal is to understand this detrimental phenomenon and develop robust processes to ensure ductile components. The results of the studies from the conventional metallographic evaluation and Auger analysis are presented.

INTRODUCTION

Phosphorus alloyed sintered steels are characterized by a unique combination of strength and ductility. The beneficial effect of alloying with phosphorus can be explained by the following three mechanisms [1]:
a) Liquid phase sintering - a transient liquid phase is formed at 1050°C by the peritectic reaction $Fe_3P + \alpha \rightarrow L$, which facilitates diffusion and densification during sintering.
b) Ferrite stabilization: phosphorus stabilizes ferrite and thereby a transformation from austenite to ferrite occurs as phosphorus diffuses into the iron particles during sintering. Since the diffusivity in ferrite is much higher than in austenite, the sintering gets more effective leading to reduced porosity and rounder pores.
c) Solid solution hardening: small amount of phosphorus in iron has a strong solution hardening effect and contributes to the high strength of phosphorus alloyed sintered steels.

The excellent ductility of Fe-P P/M steels requires that certain material and process parameters are fulfilled. Otherwise, P/M components made from phosphorus containing materials may display intergranular cracking due to weakening of the grain boundaries. Graphite addition (0.5-1 wt %) in the Fe_3P used for the powder mix has been shown to prevent brittleness in Fe-P sintered steels [2]. The same effect has been reported for adding minute amount of graphite (up to 0.07 wt %) to the powder mix for the P/M alloy FY4500 [3, 4].

For a long time, the root cause for embrittlement has been difficult to identify because there is "no well-established and easy-to-recognize" metallographic features associated with the intergranular cracking path. Currently available surface analysis techniques, such as Auger electron spectroscopy, capable of analyzing composition of atomic layers adjacent to the in-chamber fracture surfaces, have contributed greately to the understanding of these embrittlement mechanisms.

The purpose of this investigation is to study the phenomena responsible for the embrittlement that may occur in these materials. Fracture surfaces of Fe-P materials with and without graphite additions will be examined by Auger electron spectroscopy (AES). Furthermore, mechanical properties and microstructures from various cooling using similar Fe-P materials will be evaluated.

EXPERIMENTAL RESULTS

I. AUGER ELECTRON SPECTROSCOPY (AES)

The embrittlement mechanism(s) of Fe-P materials using Fe_3P without graphite addition and followed by the ones with graphite addition were investigated using AES. The samples were cleaned extensively prior to entering into the vacuum chamber. The prepared notch feature facilitates the breaking in the ultrahigh vacuum chamber prior to AES evaluation of the resultant fracture surface.

The Auger mapping of selected areas was performed on various elements - iron (Fe), phosphorus (P), oxygen (O), manganese (Mn), sulfur (S) and carbon (C). For a better understanding, the topographical view of the corresponding area was also recorded through secondary electron image (SEI). In-situ chemical composition and depth profile by ion bombardment for several conditions were also carried out and reviewed.

A. Materials without graphite addition

Figure 1 presents an area of the fracture surface of a Fe-P material displaying a brittle behaviour, together with the corresponding Auger maps of three elements Fe, P, and O. In the middle of this area several intergranular facets are visible. They appear to be part of a sintered powder particle.

In an Auger elemental map: a) bright means the area is rich in that element. b) oxygen-rich implies the area is the original as-sintered pore surface. c) oxygen-lean implies the area is the new fracture surface created in the vacuum chamber

From Auger maps, it reveals that all intergranular facets are freshly formed in AES vacuum chamber when compared to the as-sintered pore surface since all these intergranular facets are lean in O and rich in P and Fe, while the as-sintered pore surface is oxygen rich.

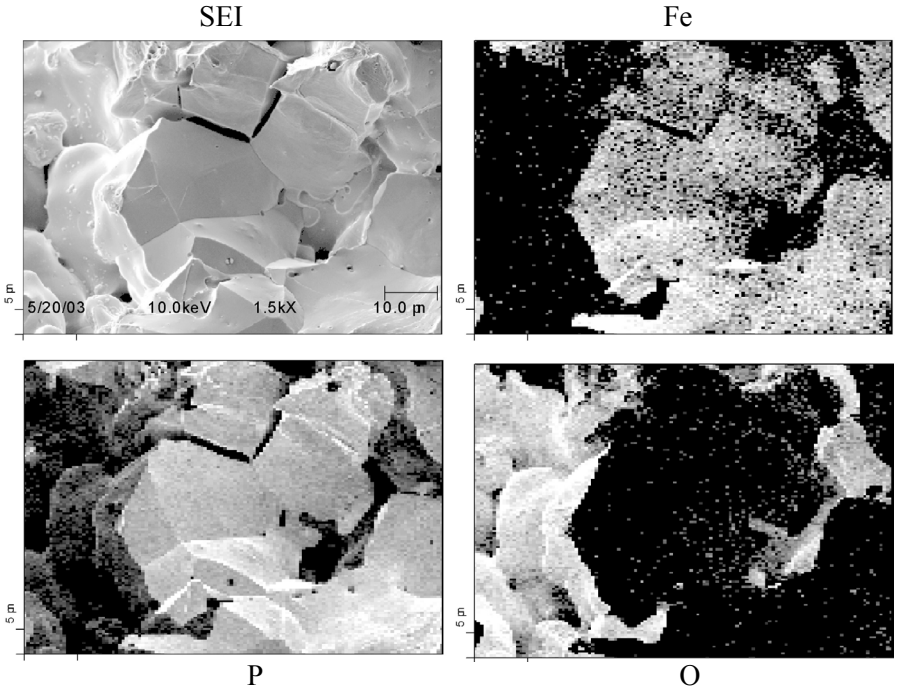


Figure 1. Materials without graphite – secondary-electron image (SEI) fractograph with Auger mapping of Fe, P and O showing intergranular facets within the particle are richer in P and Fe

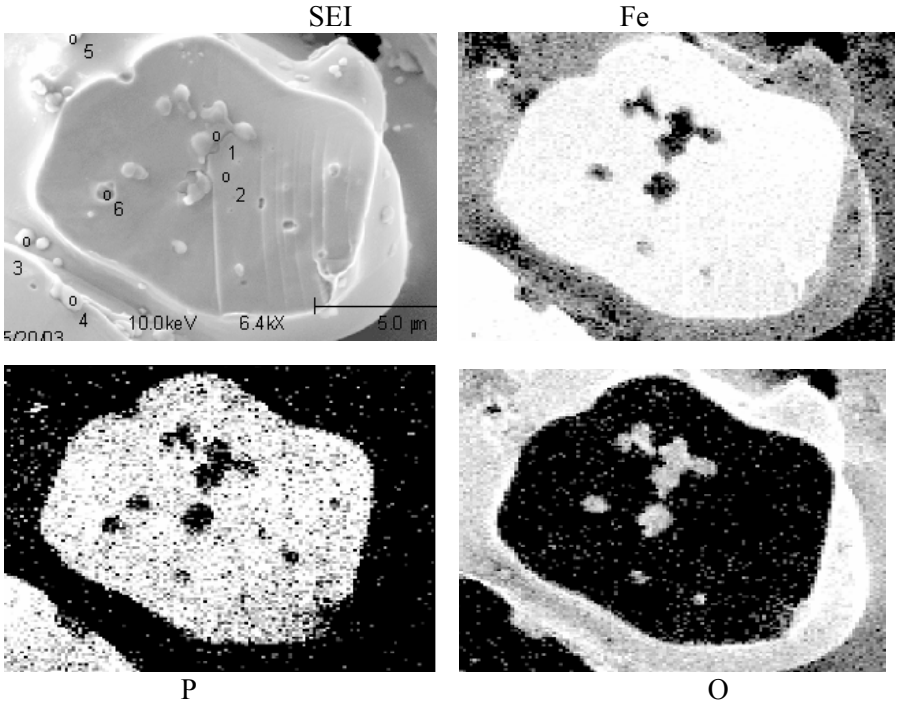


Figure 2. Materials without graphite – SEI fractograph with Auger mapping of Fe, P and O, while all the particles, independent of their location, are rich in Mn and O

Another graphite-free sample, **Figure 2**, reveals the presence of particles on the intergranular facet as well as on the adjacent as-sintered pore surface. The results indicate that the intergranular facet is rich in P and Fe. All particles on fracture surface (1,6) and on as-sintered pore surface (3,4,5) are rich in manganese besides oxygen.

In-situ concentrations profiles of Fe, P, C, and O at Point 1 in **Figure 3**, are plotted in **Figure 4**. The profile represents the concentration of a certain element measured at different depths, by removing the materials layer by layer through ion bombardment. The concentration profile in **Figure 4** indicates it is a continuous film, rich in P and Fe, of approx. 40 Angstroms (Å, 10^{-10} meter) thick**.** High C level is caused by hydrocarbon build-up on the surface over time.

The above AES results reveal that on the intergranular facets, significant amount of phosphorus preferentially segregates to the grain boundaries, forming a continuous film rich in P and Fe, when compared to the overall concentration.

B. Materials with graphite addition

The result of adding graphite is presented in **Figures 5 and 6.** Ductile features are visible in the fracture surfaces with few exceptions. Due to the relatively brittle nature of this P/M material and high impact loading, cleavage feature is acceptable as long as the fracture path is not following the grain boundary giving rise to the so-called intergranular cracking.

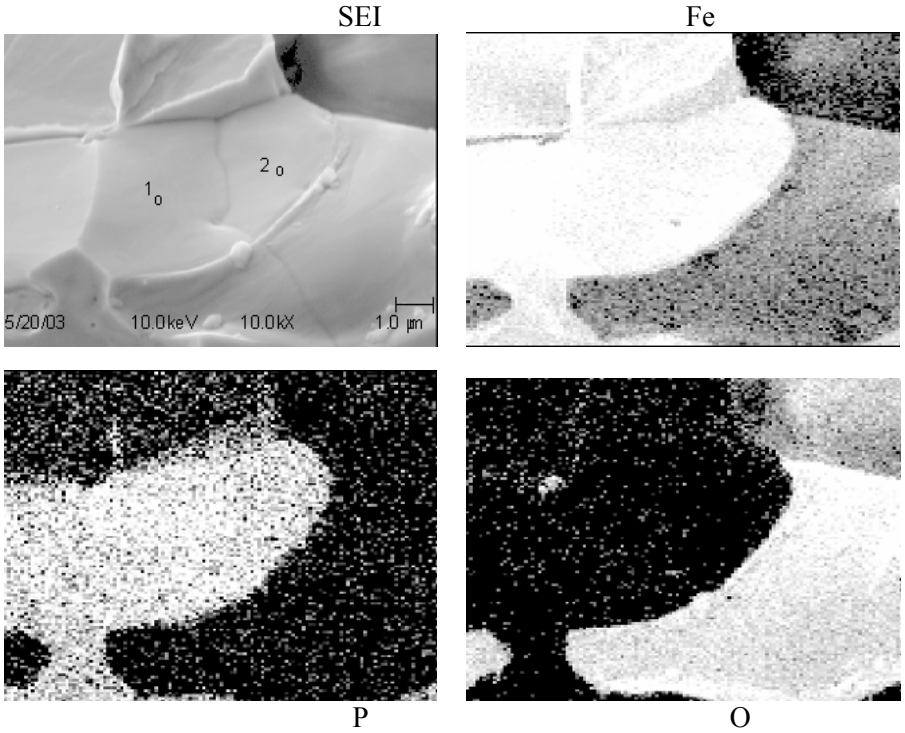


Figure 3. Materials without graphite– SEI fractograph with Auger mapping of Fe, P and O. Areas 1 and 2 are intergranular facets (part of the fracture surface) formerly two adjacent grains while the area to the right is the as-sintered pore surface. The observation is based on the appearance and the oxygen level.

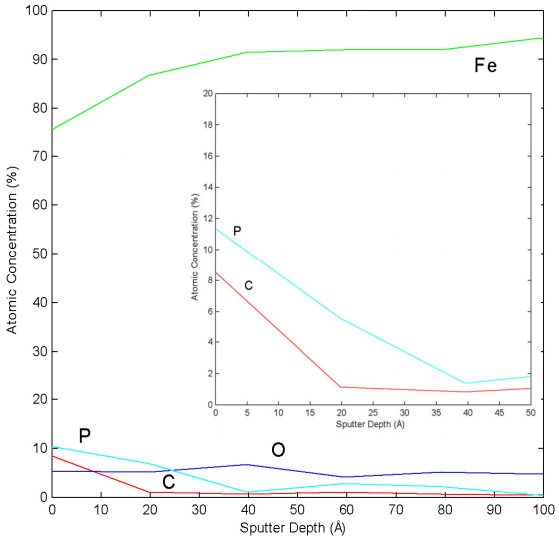


Figure 4. Concentrations-depth profile at Point 1 in **Figure 3** for Fe, P, C and O, showing the continuous film is about 40 Å thick

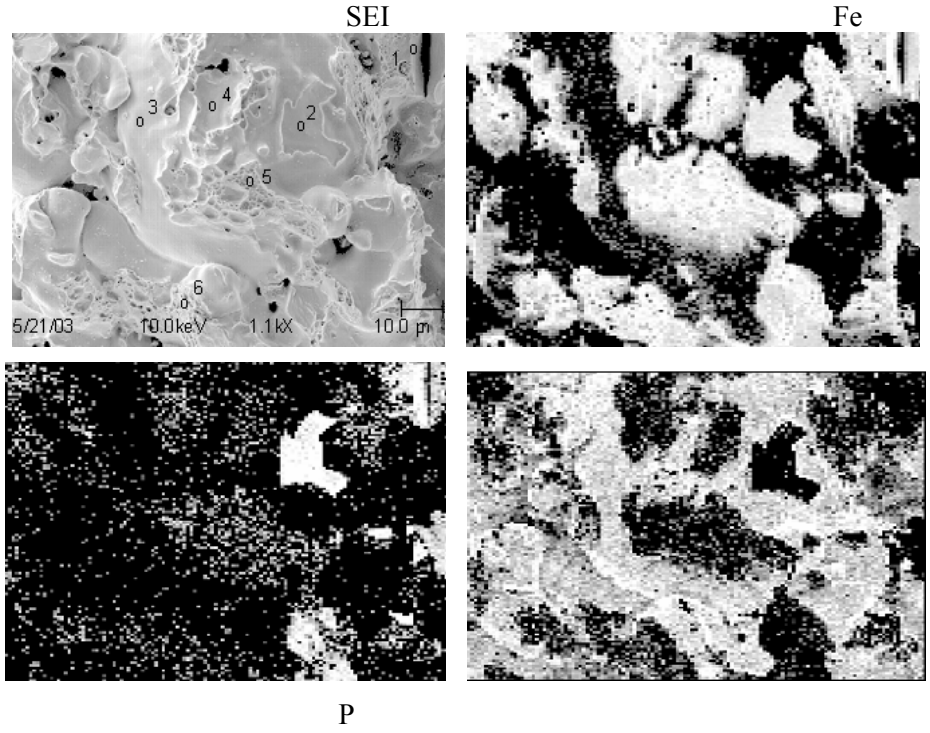


Figure 5. Graphite-added sample - SEI fractograph with Auger mapping of Fe, P and O, showing ductile features in the fracture surface as a result of graphite addition

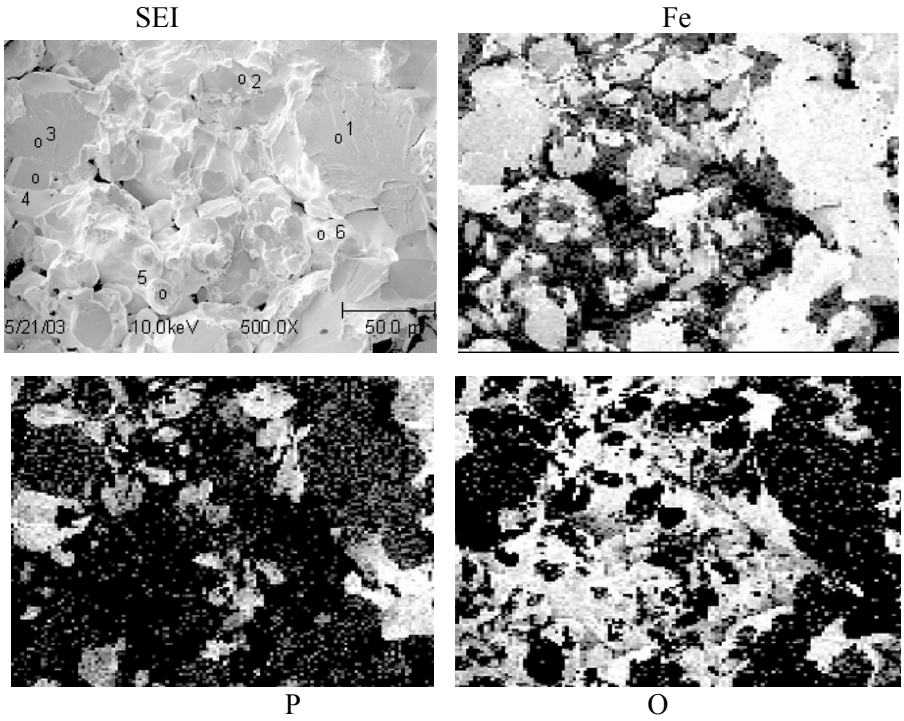


Figure 6. Graphite-added sample - SEI fractograph with Auger mapping of Fe, P and O
Cleavage features (Area 1 & 3) are visible, and acceptable, in the fracture surface

II. MECHANICAL PROPERTY AND MICROSTRUCTURE - similar materials

Two grades of Fe_3P powder were used for the investigation. Grade 1 contains 0.75 weight % combined carbon while Grade 2 has no added graphite.

Two Fe_3P lots were blended with water atomized iron powder (ASC100.29) to reach 0.45% P by weight. Amide wax of 0.8 wt % was added as lubricant. The material containing Fe_3P Grade 1 is coded 45P-1 and the material containing Fe_3P Grade 2 is coded 45P-2.

A. Processing condition

Standard bars for tensile and impact tests were compacted at 600 MPa. Sintering was performed in a laboratory belt furnace at 1120ºC (2048ºF) for 30 minutes in 90/10 N_2/H_2 atmosphere with a subsequent cooling rate of 0.8ºC/S (1.4ºF/S) from 700ºC (1292ºF) througho 400ºC (752ºF). Tensile test, Charpy impact test, and hardness measurement were performed on the sintered specimens.

Cylindrical specimens (6 mm diameter) for dilatometer runs were produced with 600 MPa compaction pressure. The lubricant in the green compacts was removed at 800°C for 60 minutes in dissociated ammonia. Sintering of the specimens was performed in a dilatometer. Heating rate was 0.5°C/S (0.9°F/S), sintering temperature 1120°C (2048ºF), time at temperature 30 minutes, and atmosphere N_2/H_2 (90/10) in all experiments. Different cooling rate in the range of 0.1-1.5°C/S (0.2- 2.7ºF/S) was applied.

B. Chemical composition

The results of chemical analyses on sintered samples are listed in **Table 1**. Oxygen is higher in 45P-2 material. Other differences in chemistry are insignificant. Although 45P-1 having added carbon in the Fe_3P to start with, carbon was reduced upon sintering down to the same level as 45P-2.

Table 1. Chemical composition - sintered test bars (weight %)

.

Materials	P	C	O	Cr	Mn	Si	Ti	V	Balance
45P-1	0.45	0.01	0.01	0.05	0.11	0.01	0.01	0.01	Fe
45P-2	0.47	0.01	0.05	0.04	0.12	0.03	0.02	0.01	Fe

C. Mechanical properties

Table 2 showing tensile strength (TS), yield strength (YS) and hardness (in HV10 scale) are independent of the Fe_3P type used for the present study. However, elongation (E) and impact strength (IE) for 45P -1 material are better than those for 45P-2 material.

Table 2. Dimensional change (green to as-sintered), density and mechanical properties of the sintered specimens.

Material	DC (%)	SD (g/cm^3)	HV10	TS (MPa)	YS (MPa)	E (%)	IE (J)
45P-1	-0.317	7.16	114	376	267	11.6	57.1
45P-2	-0.282	7.16	116	375	267	10.9	52.8

D. Microstructures

Material 45P-1 has even-phosphorus distribution and nearly equal amount of P-rich and P-lean phases. For material 45P-2, P-lean phase dominates and P-rich phase is concentrated. Compare **Figures 7 and 8**. For both materials, fracture surface of broken IE bar showed cleavage and ductile features. Occasional brittle fracture was also present, particularly in the 45P-2 material.

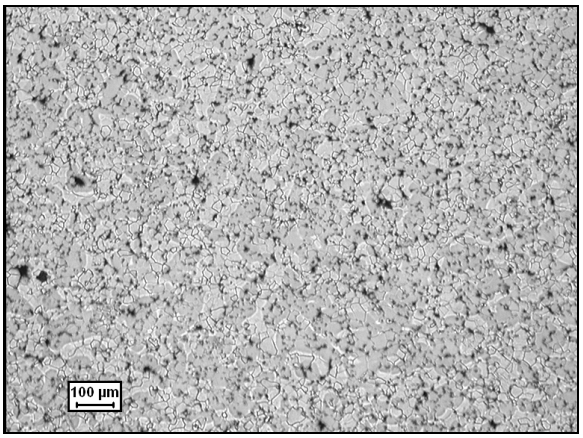


Figure 7. Microstructure of 45P-1 test bar etched in 4% Nital. Light areas are P rich and dark areas P lean.

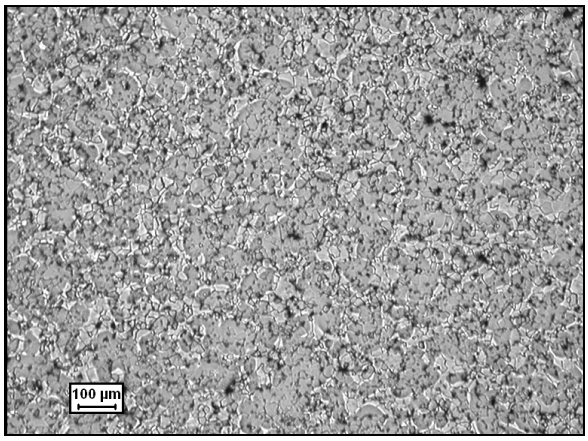


Figure 8. Microstructure of 45P-2 test bar etched in 4% Nital. Light areas are P rich and dark areas P lean.

Considerable P-segregation at grain boundary for 45P-2 material was observed in dilatometer sample cooled at rate up to 0.5°C/S (0.9°F/S). The segregation was still visible at 0.75°C/S (1.35°F/S) and disappeared beyond that cooling rate (faster cool). For material 45P-1, small sign of P-segregation at grain boundary was observed in dilatometer sample only for slow-cool at rate up to 0.3°C/S (0.5°F/S). The segregation was no longer in existence beyond that cooling rate. Compare Figures 9 and 10.

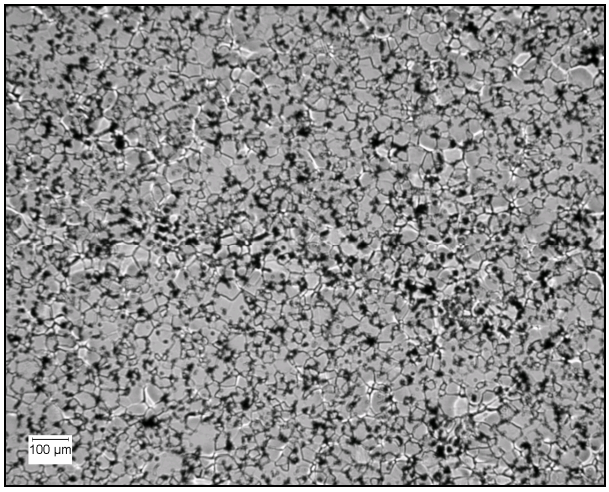


Figure 9. Microstructure of 45P-1 dilatometer specimen after cooling at 0.3°C/S (0.5°F/S), etched in 4% Nital. Light areas are P rich and dark areas P lean.

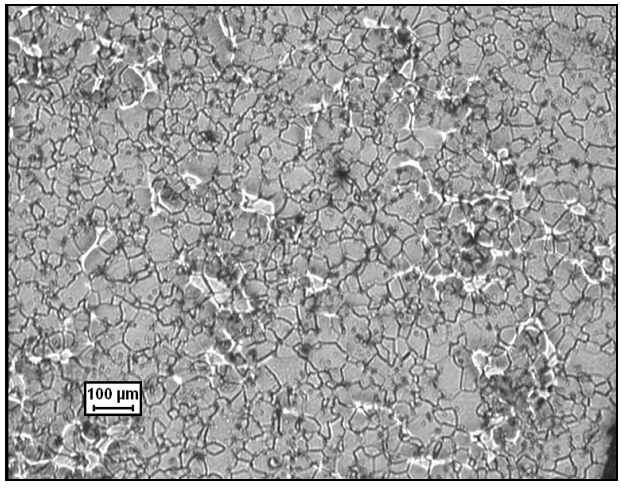


Figure 10. Microstructure of 45P-2 dilatometer specimen after cooling at 0.3°C/S (0.5°F/S), etched in 4% Nital. Light areas are P rich and dark areas P lean.

For 45P-1 material, oxides were present at grain boundary upon slow cool at rate of 0.1°C/S (0.2°F/S) and still visible at 0.3°C/S rate (0.5°F/S). Much less was observed when cooled faster (higher rate). In material 45P-2, many oxides were visible at grain boundary up to 0.5°C/S (0.9°F/S) cooling rate and still visible at high cooling rate of 0.75°C/S (1.35°F/S). Compare Figures 11 and 12.

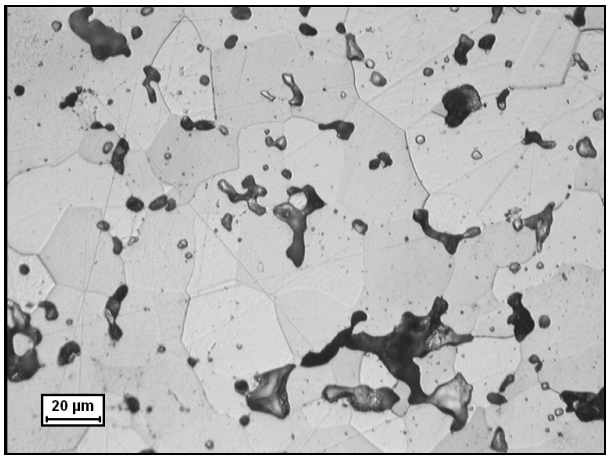


Figure 11. Microstructure of 45P-1 dilatometer specimen after cooling at 0.5°C/S (0.9°F/S), etched in 1% Nital. Few grain boundary oxides.

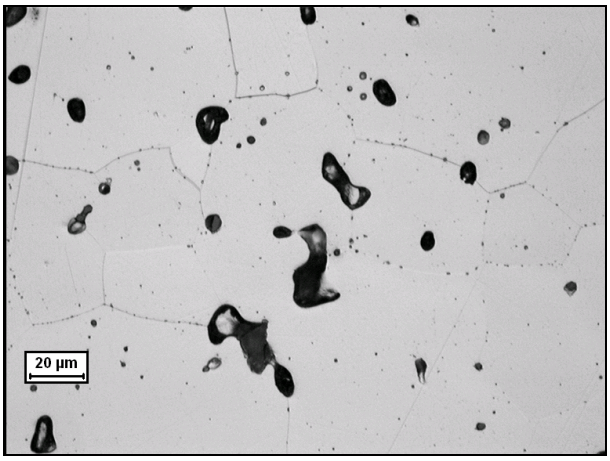


Figure 12. Microstructure of 45P-2 dilatometer specimen after cooling at 0.5°C/S (0.9°F/S), etched in 1% Nital. Many grain boundary oxides.

DISCUSSION

Brittleness due to phosphorus segregation to grain boundary during slow cool from 700°C (1290°F) down to 400°C (750°F) referred to as *temper embrittlement*, is a well-known phenomenon in low-alloyed wrought steels [5, 6]. The presence of P atoms at the grain boundary lowers the grain boundary cohesion, which leads to change in fracture mode from transgranular to intergranular. However, carbon reduces P segregation since it also has a tendency to segregate to grain boundary. Carbon atoms at the grain boundary provide higher cohesion and thereby embrittlement is prevented.

Based on the results from the AES study, the presence of continuous film at the grain boundary rich in P and Fe is the most detrimental factor causing the grain boundary to be weakened resulting in the observed intergranular cracking. The embrittling mechanism, however, is preventable.

One way to avoid the embrittlement of Fe-P sintered materials is to add a minute amount of graphite. Graphite addition to either the initial Fe_3P powder directly or the blended powder indirectly can decrease the risk of intergranular cracking in Fe-P P/M materials caused by the P segregation to grain boundary. This has been demonstrated by the results of present study.

Due to P-segregation potential under temper embrittlement, the cooling after sintering becomes an important processing step for Fe-P P/M materials. Slow cool should be avoided since they allow more time for phosphorus segregation and the formation of embrittling precipitates such as phosphides or oxides at the grain boundaries.

The study shows the presence of various oxides at pore surface as well as internal grain boundary of Fe-P materials, both with and without added graphite. It also reveals the ill-effect of slow cool on Fe-P P/M materials.

Further AES study, however, is needed to characterize the effect of cooling rate on the phosphorus segregation as well as oxide segregation (particles vs. film). This will also clarify/establish the role of oxide particles and the existence of oxide film as one of the embrittlement mechanisms.

CONCLUSIONS

- Auger Electron Spectroscopy confirms intergranular cracking caused by the P/Fe-rich continuous film existed at grain boundaries

- It also re-confirms graphite addition ensuring ductile components of Fe-P P/M materials

- Graphite can be added directly to Fe_3P powder or to the blended powder

- Avoid slow cool at rates less than 0.5°C/S in the cooling zone subsequent to sintering

ACKNOWLEDGEMENT

Research sponsored in part by the Assistant Secretary for Energy Efficiency and Renewable Energy, Office of FreedomCAR and Vehicle Technologies, as part of the High Temperature Materials Laboratory User Program, Oak Ridge National Laboratory, managed by UT-Battelle, LLC, for the U.S. Department of Energy under contract number DE-AC05-00OR22725.

Many thanks to Dr. Harry Meyer III of High Temperature Materials Laboratory in ORNL for the AES analyses. Special thanks to Scott Burrell of DaimlerChrysler for the development of the P/M cleaning procedure for Auger analysis. The coordination between Dale Wetzel of DaimlerChrysler Materials Characterization Laboratories (former assignment) and ORNL is also appreciated.

REFERENCES

1. C. Lindberg, “A new Fe-Mo-P sintered steel with extremely high impact energy”, Advances in Powder Metallurgy and Particulate Materials, Vol. 3, 1992

2. J. Tengzelius, “Avoiding brittleness in iron-phosphorus alloys”, Metal Powder Report, Vol. 48, No. 1, 1993

3. J.C. Lynn, K.S. Narasimhan, D.J. Kasputis and G. Fillari, “Processing of ferro-phosphorous-containing mixes in low hydrogen atmospheres”, 2002 Powder Metallurgy World Congress, Metal Powder Industries Federation, Princeton, NJ

4. J.C. Lynn, S.A. Burrell and P. Rosa, unpublished work at DaimlerChrysler, 2001

5. H. Erhart, H.J. Grabke, “Equilibrium segregation of phosphorus at grain boundaries of Fe-P, Fe-C-P, Fe-Cr-P, and Fe-Cr-C-P alloys”, Metal Science, Vol.15, 1981

6. H.J. Grabke, K. Hennesen, R. Möller, W. Wei, “Effects of manganese on the grain boundary segregation, bulk and grain boundary diffusivity of P in ferrite”, Scripta Metallurgica, Vol. 21, 1987